Nahrain University, College of Engineering Journal (NUCEJ) Vol.13 No.1, 2010 pp43-54

Evaluation of Reliability of Rupture and Expected Value of Fracture Speed of Ceramic Turbine Wheel Taking the Effect of Residual Stresses

Haider Hadi Jasim
Chemical Engineering Department
College of Engineering
Basrah University, Basrah, Iraq
e-mail: raidhani73@yahoo.com

Abstract

In this paper, Weibull uni-axial and multi-axial distribution function including residual stresses is developed and applied to evaluate the reliability of fracture and expected value of fracture rotating speed of turbine rotor wheel having blades manufactured from ceramic material and have inner crack. The residual stress is measured by X-Ray method. Third cases are considered, first taking only the effect of rotational loading (radial and tangential stresses) in ceramic disc, second taking the effect of rotational and thermal stresses in ceramic disc, and third taking the effect of rotational and thermal stresses in ceramic blade. As a result, there is a convergence between results gets from uni-axial and multi-axial distribution function, and the residual stresses will reduce the risk of fracture of wheel and blade. The expected values of rupture strength of ceramic blade is higher than of that of disc material, therefore the failure occurs in blade first than in disc material in service survival

Keywords: Weibull uni-axial, multi-axial distribution function, rotational stresses, residual stresses, expected rupture strength, fracture-rotating speed

Nomenclature

R_i : Inner radius of disc.

R_o : Outer radius of disc.

h: Thickness of disc.

K: Parameter Constant.

dA : Area element of the unit sphere.

dV : Volume element of unit sphere.

$S(B_o)$: Probability of survive.

B_o: Volume or surface area of a body.

m: Weibell modulus.

P_o and P: Source and integral points respectively.

u_i and t_i : Displacement and traction on a boundary node P respectively.

a_k : Rotational loading.

E: Modulus of elasticity.

y_i : Is distance vector between integral point P and the rotation axis.

ΔT : Temperature change.

$\frac{\partial T}{\partial n}$: The temperature derivative on the outer normal direction of the boundary.

T_{ij} and U_{ij} : The traction and displacement at a point in the domain for the point load considering each direction as independent.

$r_{,i}$ and $r_{,j}$: Represent the radius derivatives with respect to (x) and (y) direction respectively.

ν : Poisson's ratio.

ω : Angular velocity (rad / s).

ρ : Mass density (kg / m^3).

$\sigma_{appl.}$: Applied stress.

σ_u : Stress below which there is a zero probability of failure.

σ_o : Mean strength of material.

σ_t : Circumferential stress.

σ_r : Radial stress.

σ_{res} : Residual stress.

$E(\sigma_{max.})$: The expected value of fracture rotating speed.

μ : Shear modulus.

α : Coefficient of thermal expansion.

φ and ϕ : angle between crack and coordinates axes.

β : Beta functions.

ϕ: Title angle.

d_n and d_o :Spacing measurement at each title angle ϕ and lattice spacing.

1-Introduction

Many types of mechanical equipment contain parts revolve at high speeds under great stress, Jet engine, power generation turbine, automobile engine, turbocharger are few examples. With the recent development, the manufacture some of the part used in these equipment from ceramic material is necessary to reduce cost and improve equipment efficiency and performance.

Silicon nitride (Si_3N_4) ceramic with Y_2O_3 and $MgAl_2O_4$ additives usually used to manufacture ceramic turbine wheel having blades, due to resist high temperature and high strength [1]. For the development of ceramic turbine wheel, it becomes necessary to validation of the residual stresses and its effect on rotational strength and position of fracture origins in the rotor and blade, since the failure can be caused by the combining effect of residual and applied stresses.

Most studies on ceramic turbine wheel focused on strength or failure analysis under static loading and neglect the effect of residual stresses. Nobuo kamiya [2] develop a technique involving taking moment photographs from two and three directions at failure of ceramic radial rotor to determine the poison of crack. Takatori K. [3] find the optimum condition to fabricate silicon nitride (Si_3N_4) radial turbine wheel for gas turbine engine. Shan Lu [4] develops a new 2-D boundary element method for complex loading analysis. Yotaro Mutsuo [5] developed a new distribution function to expected values of the rupture strength of brittle rotating disc.

In this work, Weibull model is use in analysis of ceramic wheel having blade by using uni-axial and multi-axial distribution function to evaluate the reliability of ceramic disc taking account of residual stress. Three cases are taken in analysis, ceramic disc under rotation loading only, ceramic disc under rotation and thermal loading, and ceramic blade under rotation and thermal loading only.

2-Residual Stress Measured by X-Ray

Si_3N_4 ceramic turbine wheel material with Y_2O_3 and $MgAl_2O_4$ additive is brittle material, there is no ductility to accommodate plastic deformation, and this lead to that the residual stresses is resulting from the presence of elastic strain remaining in the material as a result of prior working or treatment. To determine the residual stresses, the most popular technique used is X-Ray diffraction or so called ($\sin^2\phi$) method since it is sensitive and accurate method. The residual strain is measured along radius of ceramic wheel and associated residual stresses are determined from the elastic constant assuming linear elastic distortion. The peak position of the diffraction profile was determined by one–ninth value breadth method. The wheel for measurement of X-Ray residual stress were polished with emery paper and then electro-polished. The relationship between the peak shift and residual stress is given by [6]:

$$\sigma_{res.} = \frac{E}{(1+\nu)\sin^2\phi} \times \frac{d_n - d_o}{d_o}$$

The term $(d_n - d_o)/d_o$ represents residual strain in the material. The following table listed the condition of X-Ray diffraction.

Table1. List of conditions of X-ray diffraction.

Chart speed	15 mm/min
Incident angle of X-Ray	0,18,36,45
Gonio scan speed	1 deg/min.
Divergent angle	0.35 deg.
Irradiation area	3*3 mm^2
Time constant	5 Sec
Tube current	15 mA25
Tube voltage	25 kv

Fig.1 shows turbine wheel have 14 blades. This type used for radial power turbine. Fig.2A shows method of measuring residual strain and Fig.2B shows Diffractometer apparatus. An X-Ray beam emitted from an X-Ray source in the form of point or line is directed to the sample by a slit. A Cu-target tube is generally used as the X-Ray source.

The disc piece rotates around the rotation axis in the plane of the paper so that X-Ray incidence angle α. The goniometer used shown read angle α. X-Ray detector measure the intensity of X-Ray by means of monitor scale. The Collimator used to limit the irradiated area. Filter used as absorbs and control of wavelength of X-Ray

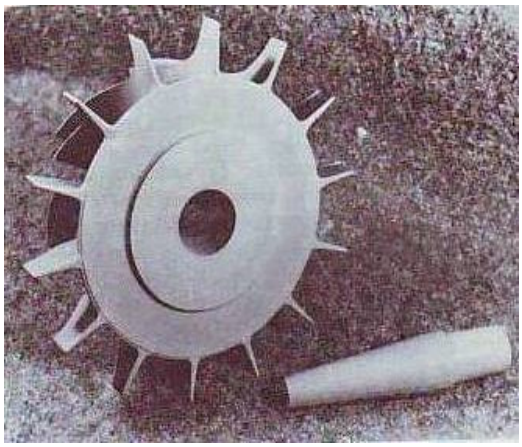

Fig.1 Ceramic turbine wheel

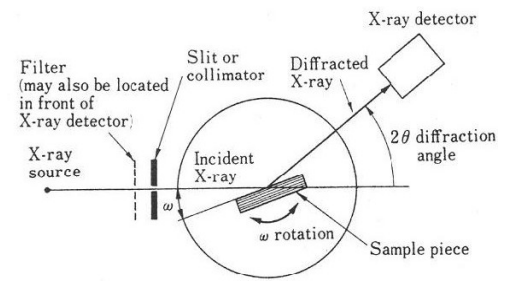

A-Method of measuring residual strain

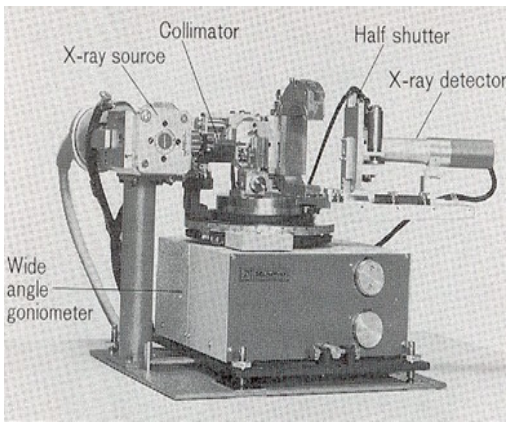

B-Diffractometer (Rigaku Co. Ltd., Japan)

Fig.2 Method of measuring using X-Ray method and Diffractometer.

3- Weibull Analysis

The key element in the design and fabrication of a component pertains it is reliability (usually determined by a safety or economic consideration), it is important to know the statistical probability of a given fracture event. According to Weibull, the two parameter distribution function $S(B_o)$ when a body subjected to a uni-axial tensile stress (σ) is given by [7] :

$$S(B_o) = e^{-B_o\left(\frac{\sigma-\sigma_u}{\sigma_o}\right)^m} \quad (1)$$

And

$$\sigma = \sigma_{appl.} + \sigma_{res.}$$

For brittle ceramic material $\sigma_u = 0$.

The risk of rupture (R) is given by:

$$R = 1 - e^{-B_o\left(\frac{\sigma}{\sigma_o}\right)^m} \quad (2)$$

Weibull also has a heuristically obtained the following multi-axial distribution function by taking the direction of the cracks at every point in the body into account for multi-axial stress state ($\sigma_1, \sigma_2, \sigma_3$) as shown in Fig.3 [7]:

$$R = 1 - e^{-\int_V (K \int_A \sigma_n^m dA) dV} \quad (3)$$

Where,

σ_n : Normal stress on the crack plane and given by:

$$\sigma_n = \cos^2\theta(\sigma_1 \cos^2\varphi + \sigma_2 \sin^2\varphi) + \sigma_2 \sin^2\theta \quad (4)$$

K: Parameter Constant and is given by the following equations:

$$K = \frac{(2m+1)}{2\pi\sigma_o^m} \quad \ldots (5)$$

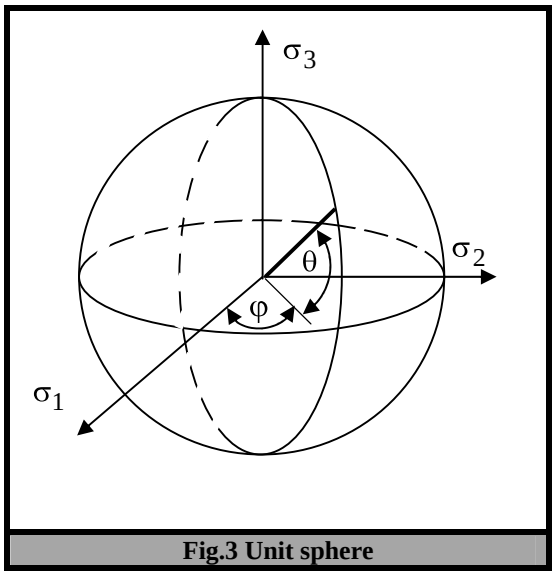

Fig.3 Unit sphere

4- The Expected Rupture Strength of a Hollow Ceramic Disc Under Rotation Loading.

For a hollow ceramic disc rotating at angular velocity (ω), the circumferential stress (σ_t) and radial stress (σ_r) given by [8]:

$$\sigma_t = \frac{\rho\omega^2}{8}[(3+\nu)(R_i^2 + R_o^2 + \frac{R_i^2 R_o^2}{r^2}) - (1+3\nu)r^2] \quad (6)$$

$$\sigma_r = \frac{\rho\omega^2}{8}(3+\nu)(R_i^2 + R_o^2 + \frac{R_i^2 R_o^2}{r^2} - r^2) \quad (7)$$

Since $\sigma_t > \sigma_r$ at any radius in the disc, and maximum circumference stress occurs at inner radius then, the maximum stress ($\sigma_{max.}$) given by:

$$\sigma_{max.} = (\sigma_t)_{r=R_i}$$

$$\sigma_{max.} = \frac{\rho\omega^2}{4}[(3+\nu)R_o^2 + (1-\nu)R_i^2)] \quad (8)$$

In the following sections, propose risk of rupture by using distribution functions described in eq.1 and eq.2

A- In the case of taking only internal cracks into consideration (uni-axial distribution function), for a hollow disc, defining the function $f_1(r)$ is:

$$f_1(r) = \frac{\sigma_t}{\sigma_{max.}}$$

$$f_1(r) = \frac{(R_o^2 + R_i^2 + \frac{R_o^2 R_i^2}{r^2}) - \frac{(1+3\nu)r^2}{(3+\nu)}}{2(R_o^2 + \frac{(1-\nu)}{(3+\nu)}R_i^2)} \quad (9)$$

And,

$$R(\sigma_{max}) = 1 - e^{-B_o(\frac{\sigma_{max}+\sigma_{res}}{\sigma_o})^m} \quad (10)$$

Where,

$$B_o = 2\pi h \int_{R_i}^{R_o} f(r)^m \, r\,dr \quad (11)$$

B- In the case of taking only internal cracks into consideration (multi-axial distribution function), defining $f_2(r)$ in a hollow disc as:

$$f_1(r) = \frac{\sigma_r}{\sigma_{max}}$$

$$f_1(r) = \frac{(R_o^2 + R_i^2 - \frac{R_o^2 R_i^2}{r^2}) - \frac{r^2}{(3+\nu)}}{2(R_o^2 + \frac{(1-\nu)}{(3+\nu)}R_i^2)} \quad (12)$$

And,

$$R(\sigma_{max}) = 1 - e^{-KB_1(\frac{\sigma_{max}+\sigma_{res}}{\sigma_o})^m} \quad (13)$$

Where,

$$B_1 = \Phi \int_{R_i}^{R_o} \int_0^{\frac{\pi}{2}} [f_1(r)\cos^2\varphi + f_2(r)\sin^2\varphi]^m \, r\,d\varphi\,dr \quad (14)$$

and

$$\Phi = \frac{4\pi h}{\beta(m+\frac{1}{2},\frac{1}{2})}$$

$$\beta(\chi,\lambda) = \int_0^1 x^{\chi-1}(1-x)^{\lambda-1}dx$$

χ and λ : constants and $\chi > 0$, $\lambda > 0$.

5- The Expected Rupture Strength of a Hollow Ceramic Disc Under Rotation and Thermal Loading.

For a hollow disc subjected at inner surface to temperature T_i and outer surface to temperature T_o, and for steady state heat flow, the temperature distribution through disc is given by [8]:

$$r\frac{dT}{dr} = c$$

$$\frac{dT}{dr} = \frac{c}{r}$$

$$T = b\ln(r) + a \quad (15)$$

Where,
a and b: Constants
r: Any radius of disc.

The radial and tangential stresses are given by the following equations [7]:

$$\sigma_r = A - \frac{B}{r^2} - \frac{E\alpha T}{2(1-\nu)} - (3+\nu)\frac{\rho\omega^2 r^2}{8} \quad (16)$$

$$\sigma_t = A + \frac{B}{r^2} - \frac{E\alpha T}{2(1-\nu)} - \frac{E\alpha b}{2(1-\nu)} - (1+3\nu)\frac{\rho\omega^2 r^2}{8} \quad (17)$$

A and B are constants determine from conditions $\sigma_r = 0$ at $r = R_i$ and at $r = R_o$.

The maximum stress occurs at inner radius and given by equations:

$$\sigma_{max.} = \sigma_t \text{ at } r = R_i$$

$$\sigma_{max} = \frac{E\alpha}{(1-\nu)(R_i^2 - R_o^2)}(T_i - T_o) + \frac{(3+\nu)}{4}\rho\omega^2 R_i^2(R_o^2+2) + \frac{E\alpha T_i}{(1-\nu)} + \frac{E\alpha b}{(1-\nu)} - \frac{(1+3\nu)}{8}\rho\omega^2 R_i^2 \quad (18)$$

The distribution function for uni-axial and multi-axial distribution is given by [2]:

$$f_1(r) = \frac{\sigma_t}{\sigma_{max}} \quad \text{and} \quad f_2(r) = \frac{\sigma_r}{\sigma_{max}}$$

Then can be used eq.11 and eq.12 for uni-axial and eq.13 and eq.14 for multi-axial distribution to determine the risk of rupture.

6- The Expected Value of Fracture Rotating Speed

The expected values of ($\sigma_{max.}$) for fracture of disc has inner crack with residual stresses can be obtain from the following equation [10]:

$$E(\sigma_{max.} + \sigma_{res.}) = \int_0^{\infty} (1 - R(\sigma_{max.} + \sigma_{res.}))d(\sigma_{max.} + \sigma_{res.}) \quad (19)$$

The expected values of (ω^2) which fracture occurs in uni-axial and multi-axial distribution function given by:

$$E(\omega^2) = \frac{4}{\rho((3+\nu)R_o^2 + (1-\nu)R_i^2)} * E(\sigma_{max.} + \sigma_{res.}) \quad (20)$$

Fig.4 show a disc specimen dimension and conditions. Table.2 shows the mechanical properties and Weibull modules used in analysis [10].

Eq.12, eq.14 and eq.20 are solving by using numerical gauss integration for precision in results.

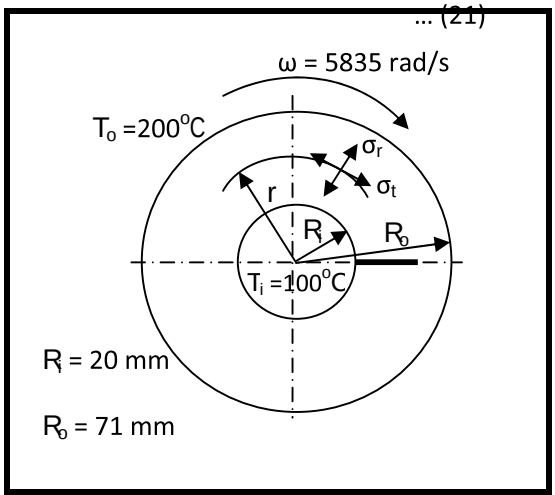

Fig.4 Disc specimen conditions

Table2. Mechanical properties of the Silicon Nitride ceramic wheel with Y_2O_3 and $MgAl_2O_4$ addition.

Quantity	constants
E	294 GPa.
ν	0.28
ρ	3210 kg / m^3
α	1.5 * 10^{-6} / ^oC
m	6.2

7- Rotational Ceramic Blade

In the case of ceramic blade subjected to rotational loading, no analytical solution is finding. Therefore, use the numerical 2-D boundary element method (BEM) to determine the maximum stress in blade for better accuracy [11, 12]. Then can be used eq.2 and eq.3 to determine the risk of rupture in blade.

The boundary integral equation of an isotropic elastic body under thermal and centrifugal loads can be expresses as [4]:

$$u_i(P_o) = \int_L [U_{ij}(P,P_o)t_j(P) - T_{ij}(P,P_o)u_i(P)]$$

$$dL(P) + \int_L [S_i(P,P_o)\Delta T - V_i(P,P_o)\frac{\partial T}{\partial n}]$$

$$dL(P) + \int_L a_i(P,P_o)dL(P)$$

And,

$$T_{ij}(P,P_o) = \frac{-1}{4\pi(1-\nu)r}\{\frac{\partial r}{\partial n}[(1-2\nu)\delta_{ij}$$

$$+ 2r_{,i}\, r_{,j}] + (1-2\nu)(n_i r_{,j} - n_j r_{,i})\}$$

$$U_{ij}(P,P_o) = \frac{1}{8\pi\mu(1-\nu)} *$$

$$[-(3-4\nu)\ln\frac{1}{r}\delta_{lk} + r_{,i}\, r_{,j}]$$

$$r_{,l} = \frac{\partial r}{\partial x}$$

$$r_{,k} = \frac{\partial r}{\partial y}$$

$$S_i = \frac{-\alpha(1+\nu)}{4\pi(1-\nu)}[(\ln r + \frac{1}{2})n_i + \frac{\partial r}{\partial n}r_{,i}$$

$$V_i = \frac{-\alpha(1+\nu)}{4\pi(1-\nu)}[(\ln r + \frac{1}{2})r_{,i}\, r$$

$$a_i = \frac{-\rho\omega^2 r}{8\pi\mu}\{(2\ln r + \frac{1}{2})[\frac{\partial r}{\partial n}y_i -$$

$$\frac{1}{2(1-\nu)}y_j r_{,j}\, n_i] - \frac{1-2\nu}{2(1-\nu)}rn_i \ln r\}$$

Fig.5 shows silicon nitride ceramic blade mesh by using 60 elements for analysis.

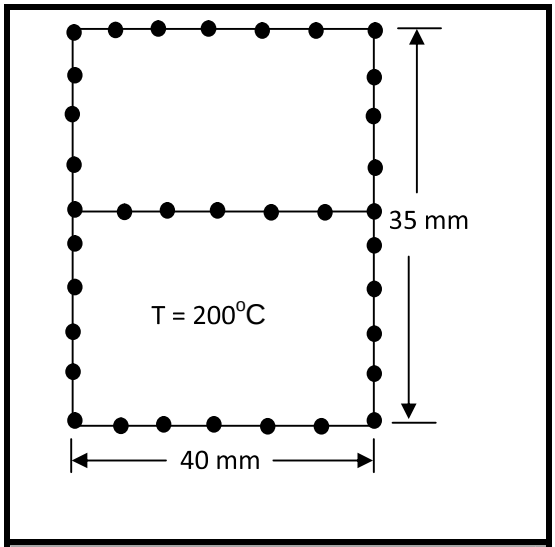

Fig.5 Boundary element mesh for blade and dimensions.

8- Result and Discussions

The residual stresses measurements at different distance in radial directions for the blade and for the wheel are shown in the Table 3 and Table 4 respectively. As shown the residual stresses in wheel vary from compressive to tension. This variation due to primary processing and surface finishing methods. A maximum value of the compressive residual stress was record at the center of disc and decrease in magnitude in direction a way from center of disc, this understood from fact that the crack initiation and propagation causes a weak residual stress failed at the crack front. The compressive residual stresses in wheel are higher comparing to that of blade.

Fig.6 shows the risk of rupture (probability of failure) for ceramic disc under rotational loading only. The curves are obtained by drawing the risk of rupture gets from eq.10 and eq.12, as shown there is a good agreement between them. The residual stresses reduce the risk of failure, this attributed to that the residual stresses are compressive and increase the strength of material.

Fig.7 shows the expected values of rupture of rotating speed against radius. It can be seen the fracture speed decrease with increasing radius. As indicated the expected values of $E(\omega^2)$ is remain constant near the outside radius.

Fig.8 and Fig.9 show the risk of rupture and expected values of rupture rotating speed under rotation and thermal loading. As shown the expected values of $E(\omega^2)$ is increase with increasing radius this because the effect of thermal loading.

Fig.10 and Fig.11 show the risk of rupture and expected values of rupture rotating speed under rotation and thermal loading for ceramic blade. These values are calculates for $\sigma_{max.} = 657.6MPa$ which gets from boundary element method. As indicated the values of $E(\omega^2)$ is larger from that for ceramic disc.

Table 3. Residual stress measurement by X-Ray method for blade.

Thickness of blade (mm)	Residual stresses (MPa.)
8	-28
16	-25
24	-19
32	-8
40	-6

Table 4. Residual stress measurement by X-Ray method for a disc.

Distance from center of wheel (mm)	Residual stresses (MPa)
40	-60
50	-53
60	-48
70	-43
80	-32
90	-17
100	-10
110	-6
120	-3
130	1
142	4

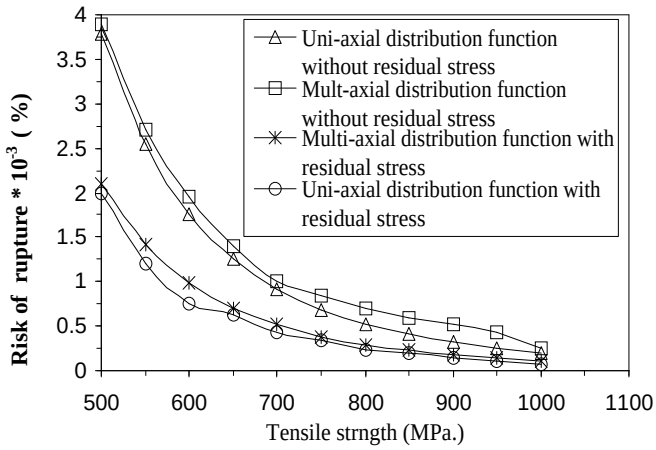

Fig.6 Risk of rupture for ceramic disc under rotation loading only.

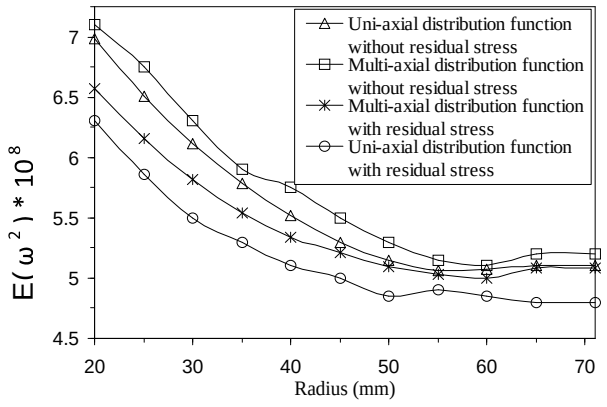

Fig.7 Expected values of ω^2 for ceramic disc under rotation loading only.

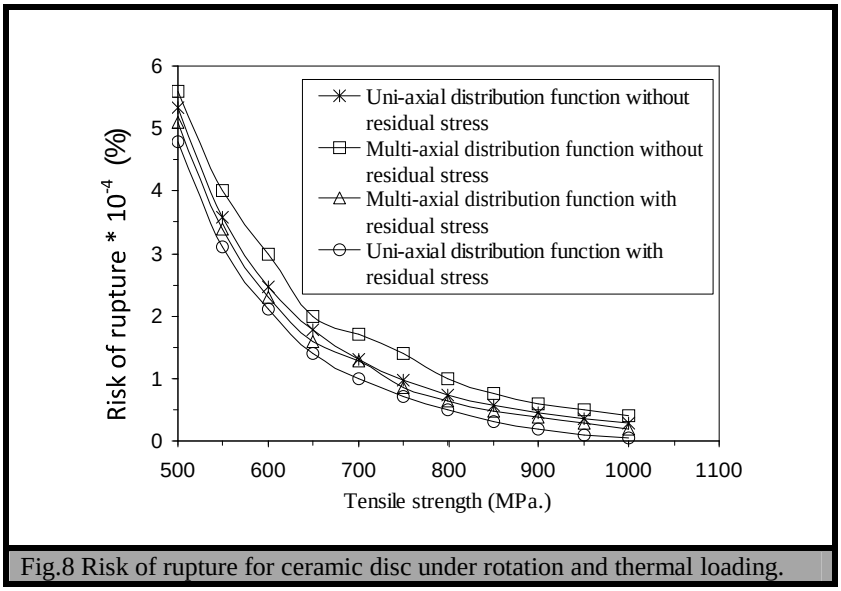

Fig.8 Risk of rupture for ceramic disc under rotation and thermal loading.

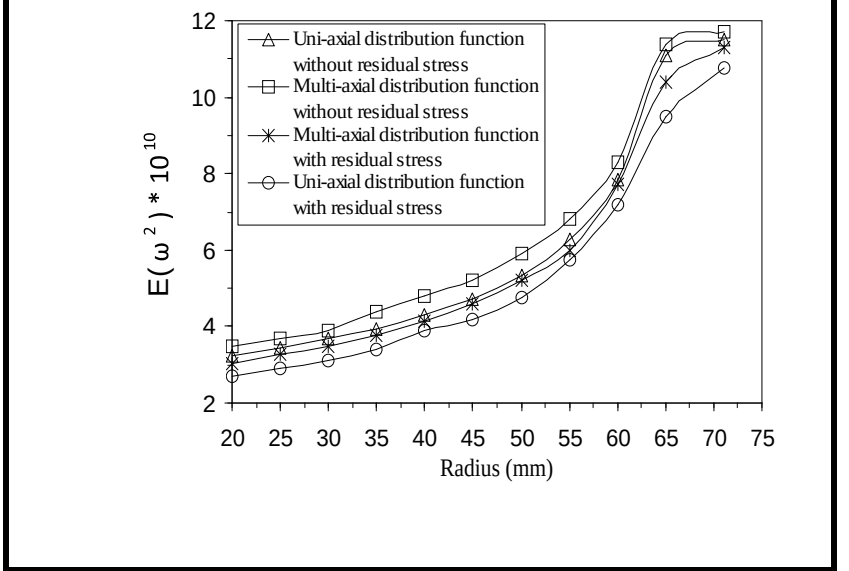

Fig.9 Expected values of ω^2 for ceramic disc under rotation and thermal loading.

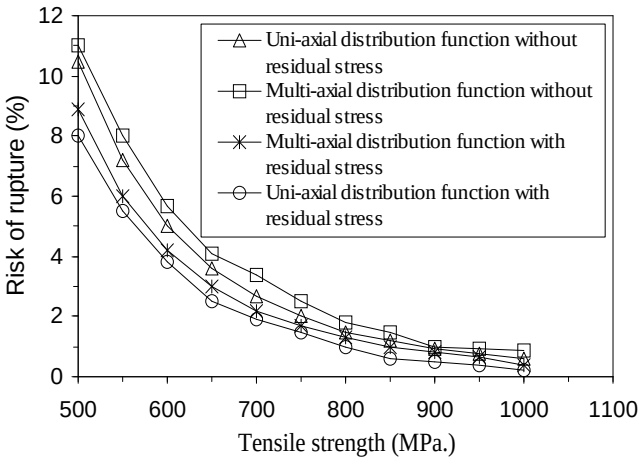

Fig.10 Risk of rupture for ceramic blade under rotation and thermal loading

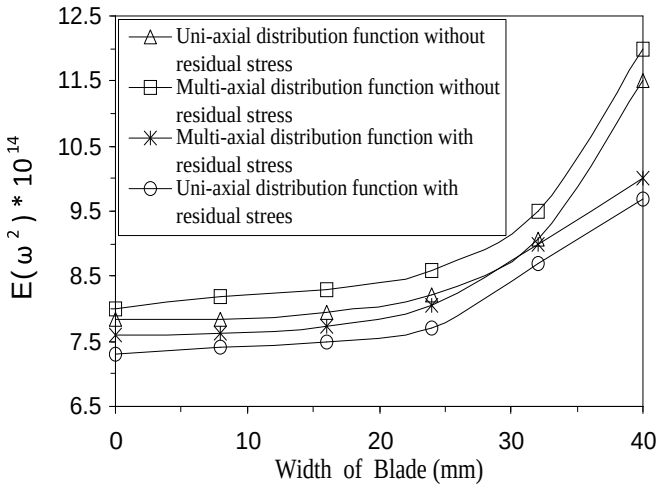

Fig.11 Expected values of ω^2 for ceramic blade under rotation and thermal loading.

9- Conclusions

From previous discussion, the following conclusions are obtained:

1- The risk of rupture and expected values of (ω^2) under rotation and thermal loading is less then that under rotation loading for ceramic disc.

2- The expected rupture strength of ceramic blade is higher than of that of disc material; therefore, the failure occurs in blade first than in disc material in service survival.

3- The existing residual stresses will reduce both risk of rupture and expected values of fracture rotating speed.

4- The extension of crack develops a relatively weaker residual stress at the crack front, this leads to decrease the magnitude of residual stress.

Acknowledgement

The author express thanks to staff engineers at Al-Zabier electrical generation station, Basrah for provide the ceramic disc sample for test and testing it, the laboratory of the material science department, Baghdad University for useful help and notes on this paper..

References

[1] Nobu Kamiya, Kenichiro Takama, Syoji Saski, Tetsuji Shimizu, "Design and evaluation of silicon nitride turbocharger rotor", ASME paper, No.91-GT-258, 1991.

[2] Nobu Kamiya, Mitsuru A., Akinobu B., and Shigetaka W., "Determination of fracture origin in ceramic radial rotor by taking photographs at failure from two or three direction", ASME paper, No.90-GT-383, 1990.

[3] Takatori K., Honma T., Kamiya N., Masak H., sasaki S., Wada S., "Fabrication and testing of ceramic turbine wheel ", ASME paper , No.91-GT-142, 1991.

[4] Shan Lu and Menhong Dong "An advanced BEM for thermal and stress analysis of components with thermal barrier coating", Electronic journal of boundary element method, Vo.1, No.2, pp.302-3015, 2003, China.

[5] Duffy S., Baker E., Wereszcsak A., and Swab J. "Weibull analysis effective volume and effective area for ceramic C-Ring test specimen", ASTEM Journal of testing and evaluation, Vo.33, No.4, 2005.

[6] Hilley M. "Analysis of residual stresses", Catalog of H and M analytical service, Inc., 2004.

[7] Yotaro Matsuo and Hideyuki Sato "A probabilistic treatise of rupture of brittle rotating disc", Bulletin of the JSME, Vo.22, No.172, 1989.

[8] Hearn E. J., "Mechanics of Material", Pergamon International Library, 1979.

[9] Lin H. T., Ferber M. K., Westphal W., and Macri F. " Evaluation of mechanical reliability of silicone nitride vanes after field tests in an industrial gas turbine", ASME GT 2002-30629, Proceedings of ASME, Turbo Expo 2002, June 3-6, 2002, Amsterdam, Netherlands.

[10] Dusza J., Lube T., Danzer R. and Weisskopf K-L "Mechanical properties of some Si_3N_4 automotive gas turbine rotor ceramics", Key engineering materials, Vo. 89, No. 91, pp.535-540, 1994.

[11] Dretta E, Francissco J. S., and Rossana V., ''The variational indirect boundary element method: A strategy toward the solution of very large problems of site response", J. of computational a caustics, vol.9, no. 2, pp. 531-541, 2001.

[12] Kesseli J., Sullivan S. S., Duffy S. F., Baker E. H., and Ferber M. K., Jonkowski J., "Comparative materials evaluation for a gas turbine rotor", 27th Annual Conference on composite, Material , and Structures, Cocoa Beach FL, 2006.

تقييم احتمالية الانكسار والقيمة المتوقعة لسرعة الانكسار لقرص تربيني دوار اخذين بنظر الاعتبار تأثير الاجهادات المتبقية

حيدر هادي جاسم
قسم الهندسة الكيماوية/ كلية الهندسة/ جامعة البصرة

الخلاصة:
في هذا البحث، دوال ويبل أحادية التوزيع للبعد ومتعددة التوزيع للإبعاد طورت من اجل حساب احتمالية الفشل واحتمالية مقاومة الانكسار لقرص تربيني دوار مصنوع من مواد سيراميكية مزود بريش يحتوي على شق داخليه اخذين بنظر الاعتبار وجود الاجهادات المتبقية. الاجهادات المتبقية تم قياسها باستخدام طريقة أشعة اكس. تم اخذ ثلاث حالات دراسية، الحالة الأولى القرص معرض إلى اجهادات دورا نية فقط، الحالة الثانية القرص معرض إلى اجهادات دورا نية وحرارية، الحالة الثالثة ريشة تربين معرضة إلى أحمال دورا نية وحرارية فقط. لقد أظهرت النتائج تقارب في القيم الناتجة باستخدام دوال ويبل أحادية التوزيع للبعد ومتعددة التوزيع للأبعاد، وان الاجهادات المتبقية سوف تقلل احتمالية الانكسار والفشل للقرص والريشة معا. القيمة المتوقعة لانكسار نتيجة السرعة الدورانية للريشة أعلى بكثير مما في القرص، لذا فان الفشل يحدث في الريشة ثم في القرص في التطبيق العملي.